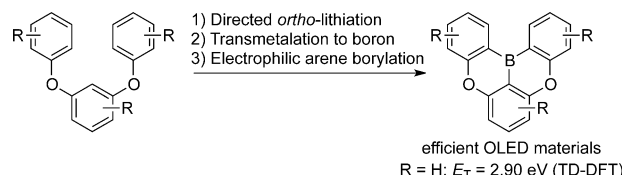


# One-Step Borylation of 1,3-Diaryloxybenzenes Towards Efficient Materials for Organic Light-Emitting Diodes

Hiroki Hirai, Kiichi Nakajima, Soichiro Nakatsuka, Kazushi Shiren, Jingping Ni, Shintaro Nomura, Toshiaki Ikuta, and Takuji Hatakeyama\*

**Abstract:** The development of a one-step borylation of 1,3-diaryloxybenzenes, yielding novel boron-containing polycyclic aromatic compounds, is reported. The resulting boron-containing compounds possess high singlet-triplet excitation energies as a result of localized frontier molecular orbitals induced by boron and oxygen. Using these compounds as a host material, we successfully prepared phosphorescent organic light-emitting diodes exhibiting high efficiency and adequate lifetimes. Moreover, using the present one-step borylation, we succeeded in the synthesis of an efficient, thermally activated delayed fluorescence emitter and boron-fused benzo[6]helicene.

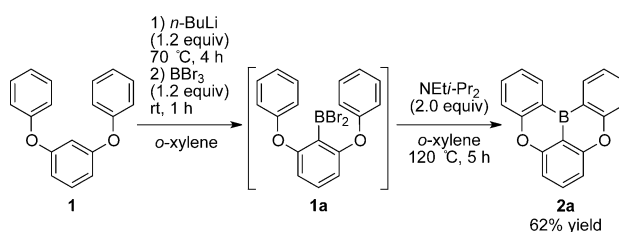
Boron-containing aromatic compounds are an important class of materials for dyes, sensors, and optoelectronics, and thus have been an attractive synthetic target for the last few decades.<sup>[1]</sup> Most boron-containing compounds have been synthesized by conventional transmetalation approaches, with organoboron compounds being readily prepared from their corresponding organolithium, -magnesium, -tin, and -silicon compounds.<sup>[2]</sup> However, preparation of organometallic compounds often requires multiple steps, and is not ideal for the generation of compound libraries or large-scale industrial production. Transition-metal-catalyzed C–H borylation<sup>[3]</sup> is potentially useful for incorporating boron atoms into aromatic skeletons, but has not yet been studied in detail. An alternative approach is electrophilic arene borylation<sup>[4]</sup> to directly convert aromatic C–H into C–B. However, directing heteroatoms, such as nitrogen<sup>[5]</sup> and oxygen,<sup>[6]</sup> are required for the construction of boron-containing polycyclic skeletons via electrophilic arene borylation. We therefore aimed to develop a one-step borylation of 1,3-diaryloxybenzenes consisting of directed *ortho*-lithiation and subsequent transmetalation to



**Scheme 1.** One-step borylation of 1,3-aryloxybenzenes.

boron, followed by tandem electrophilic arene borylation, to yield novel polycyclic aromatic compounds with a 1,4-oxaborine substructure (Scheme 1).<sup>[7]</sup> TD-DFT calculations suggest that these compounds have a large singlet–triplet ( $E_T$ ) excitation energy ( $R = H$ : 2.90 eV) owing to the localization of frontier molecular orbitals, induced by the boron and oxygen atoms (Figure 3).<sup>[8]</sup> This is a promising property for organic light-emitting diode (OLED)<sup>[9]</sup> materials. Herein, our studies into the development of a one-step borylation process, and its application for synthesis of highly efficient OLED materials, are reported. We also aim to demonstrate the versatility of the one-step borylation by a synthesis of boron-fused benzo[6]helicene.

Scheme 2 shows the optimized procedure for the one-step borylation of 1,3-diphenoxybenzene **1**: Directed *ortho*-lithiation was achieved using *n*-BuLi at 70 °C for 4 h in *o*-xylene.



**Scheme 2.** Optimized conditions for the one-step borylation.

Subsequent treatment with  $BBr_3$  gave intermediate **1a**. In the presence of two equivalents of Hünig's base, the intramolecular electrophilic borylation of **1a** took place at 120 °C to give the target borylated compound 5,9-dioxa-13b-boranaphtho[3,2,1-*de*]anthracene (**2a**) in 62 % yield. Upon examining other bases, we found that 1,2,2,6,6-pentamethylpiperidine and *N,N*-dimethyl-*p*-toluidine were as effective as  $NEt_3-Pr_2$ .<sup>[10]</sup> Notably, the reaction proceeded smoothly even in the absence of Lewis acid,<sup>[4–6]</sup> which is an efficient additive for electrophilic arene borylation. We assume that the oxygen atoms enhance the nucleophilicity of the benzene rings to

[\*] H. Hirai, K. Nakajima, S. Nakatsuka, Prof. Dr. T. Hatakeyama  
Department of Chemistry, School of Science and Technology,  
Kwansei Gakuin University  
2-1 Gakuen, Sanda, Hyogo 669-1337 (Japan)  
E-mail: hatake@kwansei.ac.jp

Prof. Dr. T. Hatakeyama  
PRESTO (Japan) Science and Technology Agency  
5, Sanbancho, Chiyoda, Tokyo 102-0075 (Japan)  
and  
ESICB, Kyoto University  
Katsura, Kyoto 615-8520 (Japan)

Dr. K. Shiren, Dr. J. Ni, S. Nomura, T. Ikuta  
JNC Petrochemical Corporation  
5-1 Goi Kaigan, Ichihara, Chiba 290-8551 (Japan)

Supporting information for this article is available on the WWW under <http://dx.doi.org/10.1002/anie.201506335>.

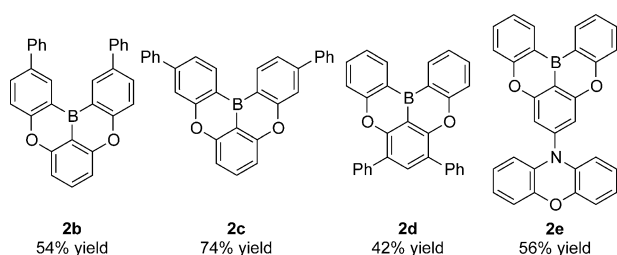


**Figure 1.** Derivatives synthesized by one-step borylation.

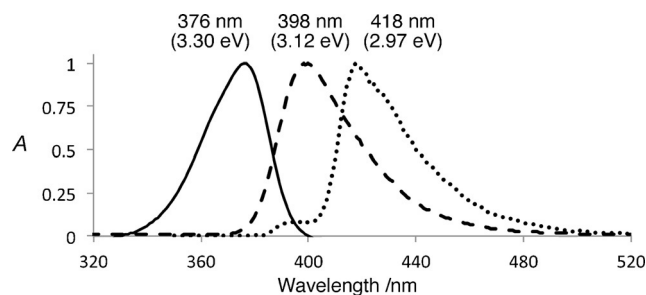


**Figure 2.** Standardized absorption (—, 0.02 mm, CH<sub>2</sub>Cl<sub>2</sub>), fluorescence (----, 0.02 mm, CH<sub>2</sub>Cl<sub>2</sub>), and phosphorescence (••••, saturated EtOH solution at 77 K) spectra of **2a**.

accelerate the borylation. Under the optimized conditions, we synthesized derivatives possessing two phenyl groups (**2b–2d**) and a phenoxazine group (**2e**) in moderate to good yields, demonstrating the versatility of the present one-step borylation (Figure 1).<sup>[10]</sup>

The UV/Vis spectrum of **2a** showed a strong absorption band corresponding to a  $\pi$ – $\pi^*$  transition with a maximum at 376 nm ( $\log \varepsilon = 4.19$ ; Figure 2), which is assignable by TD-DFT calculations to the HOMO–LUMO transition. The fluorescence spectrum showed a strong emission band at 398 nm (298 K) ( $\Phi_f = 0.62$ ; Figure 2). Interestingly, the photoluminescence spectrum showed a maximum at 418 nm (77 K; Figure 2).<sup>[11]</sup> Based on these two emission maxima, the singlet–singlet ( $E_S$ ) and singlet–triplet ( $E_T$ ) excitation energies were estimated to be 3.12 and 2.97 eV, respectively, suggesting a remarkably small energy difference ( $\Delta E_{ST} = 0.15$  eV) between the  $S_1$  and  $T_1$  states, similar to that of donor–acceptor molecules. This can be explained by the resonance effect of boron and oxygen atoms in the excited states. As shown in Figure 3, SOMO1 ( $T_1$ ), corresponding to the LUMO in the  $S_0$  state, is localized on the boron atom and at positions *ortho* and *para* to the boron atom. In contrast, SOMO2, corresponding to the HOMO in the  $S_0$  state, is localized on the oxygen atoms and at positions *meta* to boron, suppressing the exchange interaction between the SOMOs

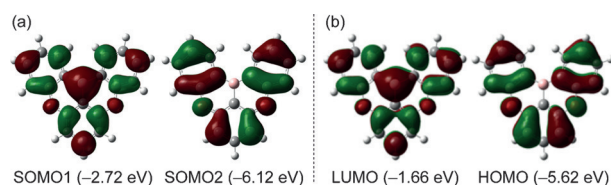


**Figure 3.** Singly occupied Kohn–Sham orbitals of **2a** in the  $T_1$  (a) and  $S_0$  (b) states, calculated at the (U)B3LYP/6-31G(d) level of theory. Orbital energies are shown in parentheses.

and minimizing the energy difference between the  $S_1$  and  $T_1$  states.<sup>[8]</sup>

The results of spectroscopic studies on the derivatives are summarized in Table 1. Despite the introduction of phenyl groups, the  $\Delta E_{ST}$  values of **2b–2d** are comparable to that of **2a** owing to localization of frontier MOs.<sup>[8]</sup> The  $E_T$  values of **2b–2d** are 2.81, 2.71, and 2.70 eV, respectively; these values are slightly smaller than that of **2a** but larger than that of 4,4'-bis(9-carbazolyl)-1,1'-biphenyl (CBP), a representative host material for phosphorescent OLEDs.<sup>[12]</sup> We also measured the ionization potentials ( $I_p$ ) of vacuum-deposited films of **2a–2d** and CBP by photoelectron yield spectroscopy, and calculated the electron affinities ( $E_a$ ) from  $I_p$  and the optical

**Table 1:** Physical properties of **2a–2e** and CBP.

|           | $\lambda_{em}^{[a]}$<br>[nm] | $E_S^{[c]}$<br>[eV] | $\Phi^{[d]}$ | $\lambda_{em}^{[b]}$<br>[nm] | $E_T^{[c]}$<br>[eV] | $I_p^{[e]}$<br>[eV] | $E_g^{[e]}$<br>[eV] | $E_a^{[e]}$<br>[eV] |
|-----------|------------------------------|---------------------|--------------|------------------------------|---------------------|---------------------|---------------------|---------------------|
| <b>2a</b> | 398                          | 3.12                | 0.72         | 418                          | 2.97                | 5.94                | 3.15                | 2.79                |
| <b>2b</b> | 410                          | 3.02                | 0.65         | 442                          | 2.81                | 6.02                | 3.00                | 3.02                |
| <b>2c</b> | 410                          | 3.02                | 0.60         | 457                          | 2.71                | 6.09                | 2.99                | 3.10                |
| <b>2d</b> | 436                          | 2.84                | 0.57         | 459                          | 2.70                | 5.90                | 2.87                | 3.03                |
| <b>2e</b> | 492                          | 2.52                | 0.92         | 477                          | 2.46 <sup>[f]</sup> | 5.50                | 2.57                | 2.93                |
| CBP       | —                            | —                   | —            | 470                          | 2.64                | 6.00                | 3.45                | 2.55                |

[a] Fluorescence measurements were carried out in CH<sub>2</sub>Cl<sub>2</sub> (0.02 mm, **2a–2d**) or on a polymethyl methacrylate (PMMA) film (1 wt%, **2e**). [b] Phosphorescence measurements were carried out in EtOH (saturated, **2a–2d**) or on a PMMA film (1 wt%, **2e**) at 77 K. [c] Singlet and triplet energies were estimated from the emission maxima unless otherwise noted. [d] Absolute PL quantum yields on a PMMA film (1 wt%). [e] Ionization potentials were determined by photoelectron yield spectroscopy (PYS). Optical band gaps were estimated from onset wavelengths of the UV/Vis absorption spectra of the vacuum-deposited thin films (**2b–2e**) or in solution (**2a**, 0.02 mm in CH<sub>2</sub>Cl<sub>2</sub>). Electron affinities were calculated from  $I_p$  and  $E_g$ . [f] Calculated from  $E_S$  and  $\Delta E_{ST}$ .  $\Delta E_{ST}$  was estimated from PL quantum yield and lifetime of the fluorescence and TADF components according to the method reported in Ref. [13f]. Fluorescence and phosphorescence lifetimes are shown in the Supporting Information.

band gaps ( $E_g$ ). The  $E_a$  values for **2a–2d** are larger than that of CBP and are suitable for carrier injection from hole- and electron-transporting layers. Introduction of a phenoxazine group (**2e**) caused a smaller red-shift at 77 K than 298 K, which is due to restriction of rotational relaxations in the excited states at 77 K. This is commonly observed in donor–acceptor molecules and makes estimation of the  $\Delta E_{ST}$  values difficult.<sup>[13]</sup> Therefore, we estimated the  $\Delta E_{ST}$  value from the quantum yield, lifetime of the fluorescence, and thermally activated delayed fluorescence (TADF) components according to Adachi's method.<sup>[13f]</sup> The estimated value was relatively small (0.06 eV), which can be attributed to the localization of frontier MOs on the 5,9-dioxa-13b-boranaphtho[3,2,1-*de*]an-

thracene or phenoxazine groups.<sup>[8]</sup> Notably, **2e** shows a much higher absolute fluorescence quantum yield ( $\Phi_f=0.92$ ). Such features are ideal for a TADF emitter.<sup>[13]</sup>

To demonstrate the potential of these derivatives as OLED materials, we prepared films of **2a–2d** by vacuum deposition, and observed rapid crystallization of **2a** and **2b**. We then prepared PHOLEDs (PH = phosphorescent) using **2c** and **2d** as host materials, with [Ir(ppy)<sub>3</sub>] (ppy = 2-(2-pyridino)phenyl) as a green dopant (Figure 4), and compared their characteristics to PHOLEDs containing CBP (Table 2, entries 1–3). PHOLEDs containing **2c** and **2d** exhibited superior performance compared to that of CBP in terms of driving voltage (*V*), current efficiency ( $\eta_c$ ), power efficiency ( $\eta_p$ ), and external quantum efficiency (EQE) at 1000 cd m<sup>-2</sup>. The small driving voltage is attributable to the higher *E<sub>a</sub>* of **2c** and **2d**, thus reducing contact resistance between the electron-transport and the emissive layers. The superior efficiencies of **2c** and **2d** may also be explained by their large *E<sub>T</sub>* values, which prevent back-transfer of energy from the dopant ([Ir(ppy)<sub>3</sub>]; *E<sub>T</sub>* = 2.50 eV). Furthermore, the lifetime of OLEDs, the most important characteristic for practical applications, was measured at an initial brightness of 2000 cd m<sup>-2</sup>. Surprisingly, the devices containing **2c** and **2d** showed significantly longer lifetimes (1000 and 383 h) than that containing CBP (95 h). The polycyclic structures of **2c** and **2d** may contribute to their substantial stability in the excited states.<sup>[14]</sup> Since derivative **2e** showed desirable fea-

tures for a TADF emitter, we prepared a device using **2e** with either **2c** or CBP as the host material. Although the device lifetimes were short (< 1 h),<sup>[15]</sup> the EQE<sub>1000</sub> values were 15.2 and 13.9%, indicating a considerable TADF contribution. These results indicate that the compounds containing 1,4-oxaborine substructures may be suitable as new classes of efficient materials for OLEDs.

To demonstrate the versatility of the one-step borylation procedure, we synthesized boron-fused benzo[6]helicene<sup>[16]</sup> **4** using 1,3-bis(naphthalen-2-yloxy)benzene **3** as a starting material (Scheme 3). The electrophilic arene borylation took place smoothly at 100 °C to give **4** in 33% yield. Notably, isomer **5** was formed in only 2% yield, suggesting that electronic effects are predominant over steric effects in the borylation step. The helical structure of **4** was confirmed by X-ray crystallography (Figure 5):<sup>[17]</sup> the B–C1 and B–C2 lengths were found to be 1.527(2) and 1.557(2) Å, respectively, indicating the single bond character. The torsion angles for each ring were 18.9° for C1–B–C2–C6, 4.6° for C6–C2–C8–C6, and 4.0° for C10–C8–C12–C14. These observations reveal the low aromatic character of BOC<sub>4</sub> rings and are consistent with the results of nucleus-independent chemical shift (NICS) analysis (NICS(0) = 0.8).<sup>[8]</sup> The optical resolution of **4** was successful, and we confirmed the activation energy for racemization to be 26.6 kcal mol<sup>-1</sup> ( $\Delta H^\ddagger$ ), which is between those of [6]helicene and [5]helicene (35.2 and 22.7 kcal mol<sup>-1</sup>, respectively).<sup>[18]</sup>

In summary, we developed a one-step borylation of 1,3-diaryloxybenzenes to yield novel polycyclic aromatic compounds with a 1,4-oxaborine substructure. The derivatives exhibit a small energy difference between the *S*<sub>1</sub> and *T*<sub>1</sub> states ( $\Delta E_{ST}$ ) because of the localization of SOMOs, induced by boron and oxygen atoms. Using these derivatives as host

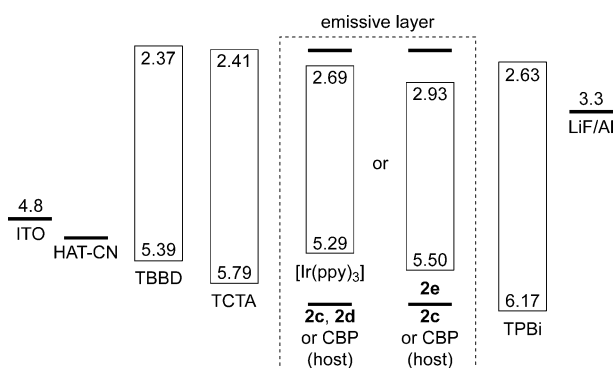
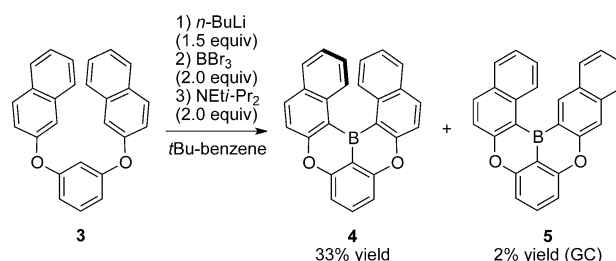


**Figure 4.** Energy diagram of the PHOLED materials (in eV). The emissive layer consists of 5 wt% [Ir(ppy)<sub>3</sub>] and 95 wt% **2b–2d** or CBP, or 20 wt% **2e** and 80 wt% **2c** or CBP. ITO = indium tin oxide, HAT-CN = dipyrazino[2,3-f':2',3'-h]quinoxaline-2,3,6,7,10,11-hexacarbonitrile, TBBD = *N,N',N'',N'''*-tetra-[1,1'-biphenyl]-4-yl)-[1,1'-biphenyl]-4,4'-diamine, TCTA = tris(4-(9*H*-carbazoyl-9-yl)phenyl)amine, TPBi = 1,3,5-tris(1-phenyl-1*H*-benzo[*d*]imidazol-2-yl)benzene.

**Table 2:** Properties of the green OLEDs.

| Entry | Host      | Dopant                  | <i>V</i> <sup>[a]</sup> | $\eta_c$ <sup>[a]</sup> | $\eta_p$ <sup>[a]</sup> | EQE <sup>[a]</sup> | LT80 <sup>[b]</sup> |
|-------|-----------|-------------------------|-------------------------|-------------------------|-------------------------|--------------------|---------------------|
| 1     | <b>2c</b> | [Ir(ppy) <sub>3</sub> ] | 5.2                     | 72.1                    | 43.5                    | 20.1               | 1000                |
| 2     | <b>2d</b> | [Ir(ppy) <sub>3</sub> ] | 5.5                     | 73.8                    | 41.9                    | 20.6               | 383                 |
| 3     | CBP       | [Ir(ppy) <sub>3</sub> ] | 5.8                     | 63.3                    | 34.1                    | 17.6               | 95                  |
| 4     | <b>2c</b> | <b>2e</b>               | 4.6                     | 52.8                    | 36.0                    | 15.2               | –                   |
| 5     | CBP       | <b>2e</b>               | 5.0                     | 40.1                    | 25.3                    | 13.9               | –                   |

[a] Driving voltage (*V*), current efficiency (cd A<sup>-1</sup>), power efficiency (lm W<sup>-1</sup>), and external quantum efficiency (%) at 1000 cd m<sup>-2</sup>. [b] Time (h) when brightness (*L*<sub>0</sub> = 2000 cd m<sup>-2</sup>) decreases to 80% (1600 cd m<sup>-2</sup>).



**Scheme 3.** Synthesis of boron-fused benzo[6]helicene.

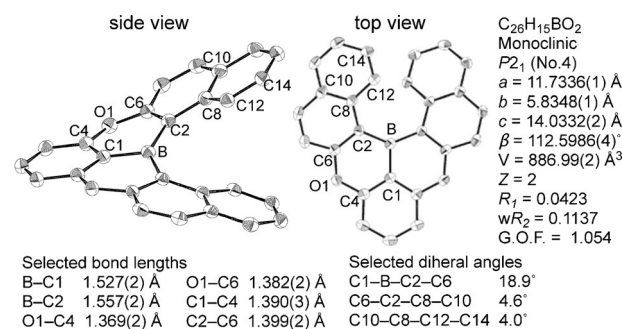


**Figure 5.** ORTEP drawing of **4**. Ellipsoids are set at 50% probability and H atoms have been omitted for clarity.



materials, we succeeded in the preparation of PHOLEDs with higher efficiencies and significantly longer lifetimes than those containing CBP. The  $\Delta E_{ST}$  was further reduced by introduction of a phenothiazine group as an efficient thermally activated delayed fluorescence (TADF) emitter. We believe that our synthetic strategy can yield a variety of boron-embedded polycyclic aromatic structures as a new class of materials for optoelectronics. Moreover, the localization of frontier molecular orbitals through the resonance effect of the heteroatom may be an alternative to the conventional donor–acceptor strategy for triplet-energy control.

## Experimental Section

A solution of *n*-butyllithium in hexane (3.28 mL, 1.60 M, 5.25 mmol) was added slowly to a solution of **1** (1.31 g, 5.0 mmol) in *tert*-butylbenzene (10 mL) at 0°C under a nitrogen atmosphere. After stirring at 70°C for 4 h, hexane was distilled off at 100°C under a continuous flow of nitrogen. Boron tribromide (0.567 mL, 6.0 mmol) was added slowly at –40°C. The reaction mixture was then allowed to warm to room temperature for 1 h and then stirred at 40°C for 1 h. After 10% of the solvent had been removed in vacuo, *N,N*-diisopropylethylamine (1.71 mL, 10 mmol) was added at 0°C. After stirring at 120°C for 5 h, *N,N*-diisopropylethylamine (0.856 mL, 5.0 mmol) was added at 0°C. The reaction mixture was then filtered with a pad of Florisil. The crude product was washed with methanol by using a sonicator to obtain **2a** (0.789 g, 58% yield, > 99% pure on <sup>1</sup>H NMR analysis) as a white solid. The filtrate was purified by preparative TLC (eluent: *n*-hexane) to obtain **2a** (46.9 mg, 3.5% yield, > 95% pure on <sup>1</sup>H NMR analysis) as a white solid. The total yield was 62% (0.836 g, > 99% pure on NMR analysis). Analytical data are reported in the Supporting Information.

## Acknowledgements

This work was supported by the Precursory Research for Embryonic Science and Technology (PRESTO) from the Japan Science and Technology Agency (JST), and a Grant-in-Aid for Scientific Research on Innovative Areas “ $\pi$ -System Figuration: Control of Electron and Structural Dynamism for Innovative Functions” (15H01004) and a Grant-in-Aid for Scientific Research (26288095) from the Ministry of Education, Culture, Sports, Science & Technology in Japan (MEXT). Synchrotron X-ray diffraction measurements were performed at the BL38B1 in the SPring-8 with the approval of JASRI (2013A1183, 2013B1083). We are grateful to Dr. Tomohiro Agou and Dr. Yoshiyuki Mizuhata (Kyoto University), and Dr. Seiki Baba (JASRI) for their support with the X-ray diffraction measurements. We are also grateful to Mr. Yohei Ono and Dr. Takeshi Matsushita (JNC Petrochemical Corporation) for their experimental support.

**Keywords:** aromaticity · borylation · helicene · light-emitting diodes · phosphorescence

**How to cite:** *Angew. Chem. Int. Ed.* **2015**, *54*, 13581–13585  
*Angew. Chem.* **2015**, *127*, 13785–13789

- [1] For reviews, see: a) F. Jäkle, *Chem. Rev.* **2010**, *110*, 3985–4022; b) H. Braunschweig, T. Kupfer, *Chem. Commun.* **2011**, 47, 10903–10914; c) N. Boens, V. Leen, W. Dehaen, *Chem. Soc. Rev.*

- 2012**, *41*, 1130–1172; d) P. G. Campbell, A. J. V. Marwitz, S.-Y. Liu, *Angew. Chem. Int. Ed.* **2012**, *51*, 6074–6092; *Angew. Chem.* **2012**, *124*, 6178–6197; e) A. Lorbach, A. Huebner, M. Wagner, *Dalton Trans.* **2012**, 41, 6048–6063; f) H. Braunschweig, I. Krummenacher, J. Wahler, *Adv. Organomet. Chem.* **2013**, *61*, 1–2; g) A. Kamkaew, S. H. Lim, H. B. Lee, L. V. Kiew, L. Y. Chung, K. Burgess, *Chem. Soc. Rev.* **2013**, *42*, 77–88; h) H. Lu, J. Mack, Y. Yang, Z. Shen, *Chem. Soc. Rev.* **2014**, *43*, 4778–4823; i) S. P. Singh, T. Gayathri, *Eur. J. Org. Chem.* **2014**, 4689–4707; j) D. Frath, J. Massue, G. Ulrich, R. Ziessel, *Angew. Chem. Int. Ed.* **2014**, *53*, 2290–2310; *Angew. Chem.* **2014**, *126*, 2322–2342; k) A. Escande, M. J. Ingleson, *Chem. Commun.* **2015**, 51, 6257–6274.
- [2] a) A. Wakamiya, K. Mishima, K. Ekawa, S. Yamaguchi, *Chem. Commun.* **2008**, 579–581; b) C. Fan, W. E. Piers, M. Parvez, *Angew. Chem. Int. Ed.* **2009**, *48*, 2955–2958; *Angew. Chem.* **2009**, *121*, 2999–3002; c) T. K. Wood, W. E. Piers, B. A. Keay, M. Parvez, *Angew. Chem. Int. Ed.* **2009**, *48*, 4009–4012; *Angew. Chem.* **2009**, *121*, 4069–4072; d) T. Agou, T. Kojima, J. Kobayashi, T. Kawashima, *Org. Lett.* **2009**, *11*, 3534–3537; e) A. Wakamiya, K. Mori, T. Araki, S. Yamaguchi, *J. Am. Chem. Soc.* **2009**, *131*, 10850–10851.
- [3] a) T. Ishiyama, N. Miyaura, *Chem. Rev.* **2004**, *3*, 271–280; b) T. Ishiyama, N. Miyaura, *Pure. Appl. Chem.* **2006**, *78*, 1369–1375; c) N. P. Mankad, *Synlett* **2014**, 1197–1201; d) A. Ros, R. Fernandez, J. M. Lassaletta, *Chem. Soc. Rev.* **2014**, *43*, 3229–3243.
- [4] a) A. M. Genaev, S. M. Nagy, G. E. Salnikov, V. G. Shubin, *Chem. Commun.* **2000**, 1587–1588; b) T. S. De Vries, A. Prokofjevs, J. N. Harvey, E. Vedejs, *J. Am. Chem. Soc.* **2009**, *131*, 14679–14687; c) A. Del Grosso, M. D. Helm, S. A. Solomon, D. Caras-Quintero, M. J. Ingleson, *Chem. Commun.* **2011**, 47, 12459–12461; d) A. Del Grosso, P. J. Singleton, C. A. Muryn, M. J. Ingleson, *Angew. Chem. Int. Ed.* **2011**, *50*, 2102–2106; *Angew. Chem.* **2011**, *123*, 2150–2154; e) A. Prokofjevs, J. W. Kampf, E. Vedejs, *Angew. Chem. Int. Ed.* **2011**, *50*, 2098–2101; *Angew. Chem.* **2011**, *123*, 2146–2149; f) V. Bagutski, A. Del Grosso, J. A. Carrillo, I. A. Cade, M. D. Helm, J. R. Lawson, P. J. Singleton, S. A. Solomon, T. Marcelli, M. J. Ingleson, *J. Am. Chem. Soc.* **2013**, *135*, 474–487.
- [5] a) T. Hatakeyama, S. Hashimoto, S. Seki, M. Nakamura, *J. Am. Chem. Soc.* **2011**, *133*, 18614–18617; b) T. Hatakeyama, S. Hashimoto, T. Oba, M. Nakamura, *J. Am. Chem. Soc.* **2012**, *134*, 19600–19603; c) X.-Y. Wang, H.-R. Lin, T. Lei, D.-C. Yang, F.-D. Zhuang, J.-Y. Wang, S.-C. Yuan, J. Pei, *Angew. Chem. Int. Ed.* **2013**, *52*, 3117–3120; *Angew. Chem.* **2013**, *125*, 3199–3202; d) X. Wang, F. Zhang, J. Liu, R. Tang, Y. Fu, D. Wu, Q. Xu, X. Zhuang, G. He, X. Feng, *Org. Lett.* **2013**, *15*, 5714–5717; e) X.-Y. Wang, F.-D. Zhuang, R.-B. Wang, X.-C. Wang, X.-Y. Cao, J.-Y. Wang, J. Pei, *J. Am. Chem. Soc.* **2014**, *136*, 3764–3767; f) S. Hashimoto, T. Ikuta, K. Shiren, S. Nakatsuka, J. Ni, M. Nakamura, T. Hatakeyama, *Chem. Mater.* **2014**, *26*, 6265–6271; g) G. Li, W.-W. Xiong, P.-Y. Gu, J. Cao, J. Zhu, R. Ganguly, Y. Li, A. C. Grimsdale, Q. Zhang, *Org. Lett.* **2015**, *17*, 560–563; h) J. M. Farrell, D. W. Stephan, *Angew. Chem. Int. Ed.* **2015**, *54*, 5214–5217; *Angew. Chem.* **2015**, *127*, 5303–5306.
- [6] a) M. J. S. Dewar, R. Diets, *J. Chem. Soc.* **1960**, 1344–1347; b) Q. J. Zhou, K. Worm, R. E. Dolle, *J. Org. Chem.* **2004**, *69*, 5147–5149.
- [7] a) J. Kobayashi, K. Kato, T. Agou, T. Kawashima, *Chem. Asian J.* **2009**, *4*, 42–49; b) L. Niu, H. Yang, Y. Jiang, H. Fu, *Adv. Synth. Catal.* **2013**, *355*, 3625–3632; c) E. Dimitrijevic, M. S. Taylor, *Chem. Sci.* **2013**, *4*, 3298–3303.
- [8] See the Supporting Information for details of the calculations.
- [9] a) C. W. Tang, S. A. VanSlyke, *Appl. Phys. Lett.* **1987**, *51*, 913–915; b) M. C. Gather, A. Köhnen, K. Meerholz, *Adv. Mater.* **2011**, *23*, 233–248; c) S. Hofmann, M. Thomschke, B. Lüssem, K.

- Leo, *Opt. Express* **2011**, *19*, A1250–A1264; d) L. Duan, J. Qiao, Y. Sun, Y. Qiu, *Adv. Mater.* **2011**, *23*, 1137–1144; e) J. Huang, J.-H. Su, H. Tian, *J. Mater. Chem.* **2012**, *22*, 10977–10989; f) Y. Chen, D. Ma, *J. Mater. Chem.* **2012**, *22*, 18718–18734.
- [10] See the Supporting Information for details of the screening. **2c** was prepared from the corresponding 2-bromo-1,3-diaryloxybenzene through the lithium–bromine exchange reaction.
- [11] Emission maximum of an EtOH solution is 397 nm at 298 K, indicating that the interaction between the boron atom and EtOH is not significant. The relatively weak emission at 390–400 nm at 77 K is determined to be fluorescence. See the Supporting Information for details.
- [12] a) Y. Ma, H. Zhang, J. Shen, C. Che, *Synth. Met.* **1998**, *94*, 245–248; b) M. A. Baldo, D. F. O'Brien, Y. You, A. Shoustikov, S. Sibley, M. E. Thompson, S. R. Forrest, *Nature* **1998**, *395*, 151–154; c) L. Xiao, Z. Chen, B. Qu, J. Luo, S. Kong, Q. Gong, J. Kido, *Adv. Mater.* **2011**, *23*, 926–952; d) A. Chaskar, H.-F. Chen, K.-T. Wong, *Adv. Mater.* **2011**, *23*, 3876–3895; e) K. S. Yook, J. Y. Lee, *Adv. Mater.* **2012**, *24*, 3169–3190; f) H. Sasabe, J. Kido, *J. Mater. Chem. C* **2013**, *1*, 1699–1707; g) C. Murawski, K. Leo, M. C. Gather, *Adv. Mater.* **2013**, *25*, 6801–6827; h) B. Minaev, G. Baryshnikov, H. Agren, *Phys. Chem. Chem. Phys.* **2014**, *16*, 1719–1758.
- [13] a) Q. Zhang, J. Li, K. Shizu, S. Huang, S. Hirata, H. Miyazaki, C. Adachi, *J. Am. Chem. Soc.* **2012**, *134*, 14706–14709; b) H. Uoyama, K. Goushi, K. Shizu, H. Nomura, C. Adachi, *Nature* **2012**, *492*, 234–238; c) J. Li, T. Nakagawa, J. MacDonald, Q. Zhang, H. Nomura, H. Miyazaki, C. Adachi, *Adv. Mater.* **2013**, *25*, 3319–3323; d) Q. Zhang, B. Li, S. Huang, H. Nomura, H. Tanaka, C. Adachi, *Nat. Photonics* **2014**, *8*, 326–332; e) H. Nakanotani, T. Higuchi, T. Furukawa, K. Masui, K. Morimoto, M. Numata, H. Tanaka, Y. Sagara, T. Yasuda, C. Adachi, *Nat. Commun.* **2014**, *5*, 4016–4023; f) Q. Zhang, H. Kuwabara, W. J. Potscavage, S. Huang, Y. Hatae, T. Shibata, C. Adachi, *J. Am. Chem. Soc.* **2014**, *136*, 18070–18081; g) S. Hirata, Y. Sakai, K. Masui, H. Tanaka, S.-Y. Lee, H. Nomura, N. Nakamura, M. Yasumatsu, H. Nakanotani, Q. Zhang, K. Shizu, H. Miyazaki, C. Adachi, *Nat. Mater.* **2015**, *14*, 330–336.
- [14] Degradation of CBP can occur by cleavage of carbon–nitrogen single bonds: a) D. Y. Kondakov, W. C. Lenhart, W. F. Nichols, *J. Appl. Phys.* **2007**, *101*, 024512–024518; b) D. Y. Kondakov, T. D. Pawlik, W. F. Nichols, W. C. Lenhart, *J. Soc. Information Display* **2008**, *16*, 37–46. For review on chemical degradation of OLED materials, see: c) S. Schmidbauer, A. Hohenleutner, B. König, *Adv. Mater.* **2013**, *25*, 2114–2129.
- [15] OLEDs based on TADF show relatively short lifetimes, which is an issue which must be solved for their use in practical applications. See reference [12].
- [16] For recent reviews, see: a) A. Rajca, S. Rajca, M. Pink, M. Miyasaka, *Synlett* **2007**, 1799–1822; b) R. Amemiya, M. Yamaguchi, *Chem. Rec.* **2008**, *8*, 116–127; c) F. Dumitrescu, D. G. Dumitrescu, I. Aron, *ARKIVOC* **2010**, *1*, 1–32; d) K. B. Jørgensen, *Molecules* **2010**, *15*, 4334–4358; e) Y. Shen, C.-F. Chen, *Chem. Rev.* **2012**, *112*, 1463–1535.
- [17] CCDC 1404513 (**4**) contains the supplementary crystallographic data for this paper. These data can be obtained free of charge from The Cambridge Crystallographic Data Centre via [www.ccdc.cam.ac.uk/data\\_request/cif](http://www.ccdc.cam.ac.uk/data_request/cif).
- [18] For calculated values, see: S. Grimme, S. D. Peyerimhoff, *Chem. Phys.* **1996**, *204*, 411–417.

Received: July 9, 2015

Revised: August 7, 2015

Published online: September 18, 2015